Molecular Dynamics Study of an Aqueous LiF Solution

Sheng-Bai Zhu and G. Wilse Robinson

SubPicosecond and Quantum Radiation Laboratory, Texas Tech University, Lubbock, TX 79409, USA

Z. Naturforsch. **46a**, 221–228 (1990); received October 4, 1990

The structure and properties of a 1.791 molal aqueous LiF solution is investigated by performing molecular dynamics simulations using a water model with both bond flexibility and instantaneously responsive polarization. On average, each cation is in close contact with about one anion. This causes a strong overlap of the hydration shells and an almost complete breakdown of the surrounding water structure. While the lone pairs of the hydration waters in the first Li^+ shell occupy preferentially tetrahedral positions, the orientational distribution of the solvent molecules around F^- is quite uniform. By comparing various autocorrelation functions of water molecules in the solution and in the pure liquid, the influence of solvated ions on the translational, rotational and vibrational motions of hydration water can be studied.

Key words: Hydration, Ions, Water, Solubility, Ion-pairs.

1. Introduction

During recent years a considerable number of computer simulations using various water models have been devoted to basic studies of the structure and properties of aqueous electrolyte solutions containing individual alkali or halide ions [1–7] or ion pairs [8–24]. These studies are of fundamental interest, since hydration of ions would be expected to perturb the local structure of liquid water, affect the transport characteristics of the ions [25, 26] and change the ionic permeability through organized structures such as biological membranes [27]. Generally speaking, these simultions have been found to be in reasonable agreement with experimental data, and, furthermore, they seem to be capable of predicting features that are not directly accessible through experimentation.

It is known that the hydrogen bond gives rise to a comparatively strong and directional intermolecular interaction. Consequently, the geometry and vibrational properties of a molecule participating in such a bond must be different from those in the gas phase. In fact, significant changes in the frequencies of the vibrational motions between nonbonded and bonded water molecules can be observed [23]. Structural and other microscopic properties of ions and water molecules in the hydration shell are influenced by these intramolecular properties [6]. The polarization effect must also play an essential role in the hydration of electrolytes [4, 28–31]. Thus, we believe that a flexible-polarizable model of water should give additional information about aqueous ionic solutions that is not available when using other water models.

In this article, we extend our previous studies on flexible and polarizable water [32] by the inclusion of lithium fluoride molecules. Lithium fluoride is small in size and mass, and is relatively insoluble ($\sim$0.1 molal) in room temperature water [33]. Previous computer simulations of this solution are mostly based on Monte Carlo methods [8, 10, 21]. Here we perform a standard NVE molecular dynamics calculation so that not only the solution structure but also a variety of relaxation processes can be investigated.

2. Molecular Dynamics System

A standard molecular dynamics simulation with periodic boundary conditions is carried out on a CRAY-YMP supercomputer for a system of eight ^7Li ions, eight ^{19}F ions, and 248 water molecules. This represents a highly supersaturated LiF solution having a molality of 1.791. The length of one side of the basic cubic cell is 19.73 Å, corresponding to a density of the solution of 1.011 g/cm^3. The temperature of the system is maintained at 298 K.

In this work, we employ the SPC-FP model [32] to mimic water molecules. This is a 3-site version with one hypothetical oxygen atom and two hydrogen atoms. These particles are linked to one another

Reprint requests to Dr. G. W. Robinson, Subpicosecond and Quantum Radiation Laboratory, P.O. Box 4260, Texas Tech University, Lubbock, TX 79407, USA.

0932-0784 / 91 / 0300-0221 $ 01.30/0. – Please order a reprint rather than making your own copy.

through harmonic intramolecular potentials including cross terms. The force constants are the same as those used by Toukan and Rahman [34]. For an unperturbed gas-phase SPC-FP molecule, the structural parameters are taken to coincide with the experimental values [35]: the equilibrium O–H bond length is 0.9572 Å and the H–O–H bond angle is 104.52°.

Any two water molecules in the system interact through a 12–6 Lennard-Jones force centered on the oxygen atom of each molecule. There are nine Coulomb forces, which are modified by the reaction field geometry with conducting boundary conditions [36]. The pairwise intermolecular potential is thus

$$U_{\text{inter}} = \sum_{i<j}^{N} \left\{ \frac{A}{r_{i0j0}^{12}} - \frac{B}{r_{i0j0}^{6}} + \sum_{l=1}^{3} \sum_{k=1}^{3} \frac{q_{il}\, q_{jk}}{r_{iljk}} \left[1 + \frac{\varepsilon_{\text{RF}} - 1}{2\varepsilon_{\text{RF}} + 1} \left(\frac{r_{iljk}}{r_c} \right)^3 \right] \right\}, \tag{1}$$

where the subscripts l and k represent O or H; q denotes the appropriate point charge; r_{iljk} is the distance between particle l of the ith molecule and particle k of the jth molecule; and $r_c = 9.863$ Å defines the cutoff radius beyond which all intermolecular interactions are truncated to zero. In accordance with the conducting boundary condition, the frequency-independent dielectric constant of the background continuum ε_{RF} is chosen to be infinity. This is acceptable for moderately to highly polar substances such as water [36]. In an SPC-FP water molecule the oxygen atom carries a negative charge and the hydrogen atoms carry positive charges, the magnitudes being chosen so as to reproduce a dipole moment of 1.83 Debye. This is the experimental value measured for the water molecule in the vapor phase [37]. These charges are fixed in position. To emulate the molecular polarization, the magnitudes of these point charges are allowed to vary according to the instantaneous local electric field and the relative orientation of the water molecule. Although more approximate, this is a considerably simpler and computationally more tractable approach than other recent polarization algorithms [38–40]. It thus allows a statistically meaningful study of locally perturbed water, which may comprise only a small part of the total ensemble. The effective polarizability 1.271 Å^3, which is somewhat lower than the free-molecule value [41] of 1.444 Å^3, has been adjusted by comparing the simulation results in the bulk phase with the available experimental data [32]. These molecular parameters are summarized in Table 1.

Table 1. Molecular parameters.

(a) Water-water interaction *

A (kcal/mol · Å^{12})	B (kcal/mol · Å^6)	q_O^0 (e)	q_H^0 (e)	α (Å^3)
695 000	600	−0.65	+0.325	1.271

(b) Ion-ion interaction

C (kcal/mol)	β (Å^{-1})	q_{Li^+}	q_{F^-}
393 581	6.32	e	−e

(c) Ion-water interaction **

ε_{LiO}	ε_{LiH}	ε_{FO}	ε_{FH}	σ_{LiO}	σ_{LiH}	σ_{FO}	σ_{FH}
0.132	0.067	0.224	0.114	2.85	2.63	3.13	2.90

* e represents the electron charge.
** ε in units of kcal/mol, σ in units of Å.

Most of the computer simulation studies reported so far for the alkali halides have been based upon the set of semi-empirical effective pair potentials obtained by Tosi and Fumi [42]. Here, for simplicity, we neglect the less important dispersion terms and write the ion pair potential in the Born-Mayer form [43]

$$U_{\text{LiF}} = C\, e^{-\beta r} - \frac{e^2}{r}, \tag{2}$$

where r denotes the ion-ion distance, and e represents the electron charge. The values of the parameters C and β are estimated from the equilibrium bond length of 1.55 Å and the ionization energy of 7.826 eV in the vapor phase [44]. Polarization effects of the closed-shell ions are not taken into account in the present work.

Equation (2) is also valid for describing the potential energy of ions belonging to different salt molecules. Unlike most earlier calculations, these ions interact individually with every atom in the water molecule. In this way, the angular dependence of the interaction is more explicitly considered. These interactions include the 12–6 Lennard-Jones force as well as electrostatic forces. Individual atom-ion interactions can therefore be expressed as

$$U_{\text{IN}} = 4\varepsilon_{\text{IN}} \left[\left(\frac{\sigma_{\text{IN}}}{r_{\text{IN}}} \right)^{12} - \left(\frac{\sigma_{\text{IN}}}{r_{\text{IN}}} \right)^{6} \right] + \frac{q_{\text{I}}\, q_{\text{N}}}{r_{\text{IN}}}, \tag{3}$$

where I represents Li^+ or F^- and N represents an oxygen or a hydrogen nucleus on the water molecule.

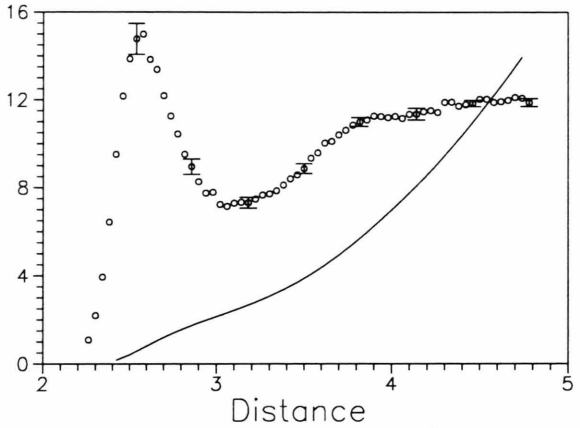

Fig. 1. Radial distribution function $g_{Li^+O}(r/\text{Å})$, and running integration number.

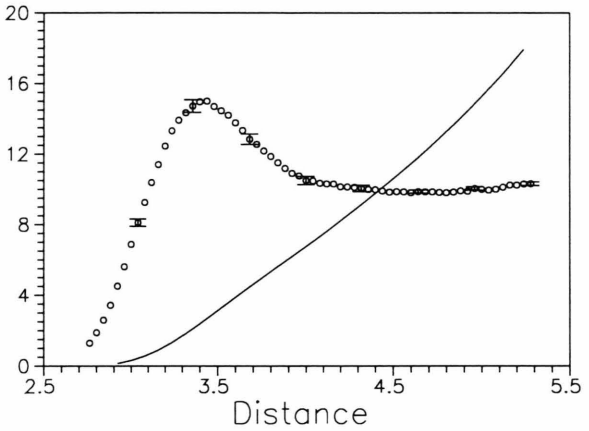

Fig. 2. Radial distribution function $g_{Li^+H}(r/\text{Å})$, and running integration number.

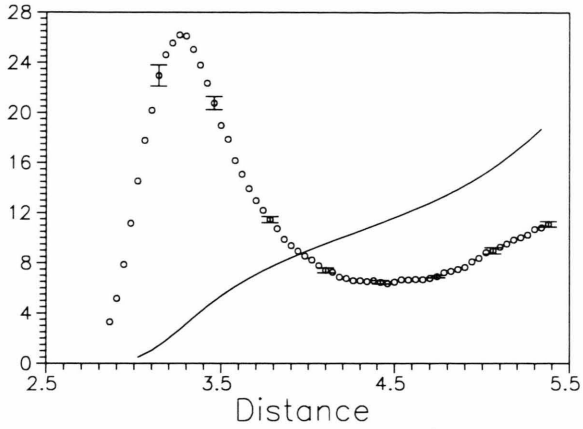

Fig. 3. Radial distribution function $g_{F^-O}(r/\text{Å})$, and running integration number.

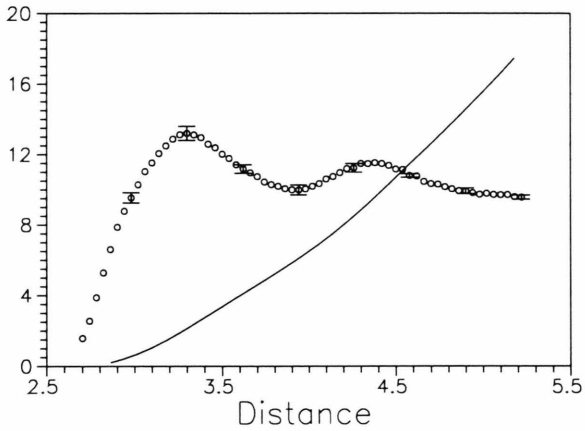

Fig. 4. Radial distribution function $g_{F^-H}(r/\text{Å})$, and running integration number.

A double time scale (0.25 fs for intramolecular degrees of freedom and 0.5 fs for intermolecular motions) is employed for better accuracy in the integration of the equations of motion. After the system equilibrates, 1.44×10^5 additional time steps are carried out to collect data. This long run is divided into 15 pieces, each of which lasts 2.4 ps and is assumed to represent an individual measure. Standard deviations of these measurements are used to determine the statistical errors [45].

3. Solvation Structure

The derivation of various radial distribution functions (RDF) from a computer simulation provides a partial description of the structure of an aqueous electrolyte solution. In Figs. 1–4, we plot the lithium-oxygen, the lithium-hydrogen, the fluorine-oxygen, and the fluorine-hydrogen RDFs, together with running integration numbers [11, 19] and the corresponding error bars. Because of the relatively short internuclear distances between the anion and the cation, some hydration shells overlap with one another. This causes an ambiguity in the determination of the coordination numbers. Partial screening, caused by the presence of an oppositely charged ion in an ionic shell, may significantly reduce the solvation structure. In particular, the first peaks of the RDFs become less pronounced than those where an isolated ion is present [3]. The first minima become congested when more than one

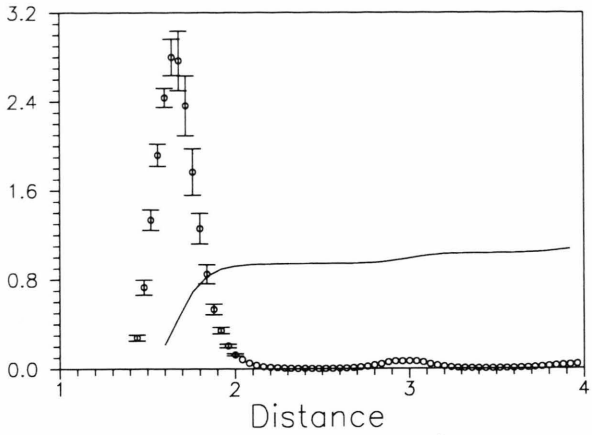

Fig. 5. Radial distribution function $g_{Li^+F^-}(r/Å)$, and running integration number.

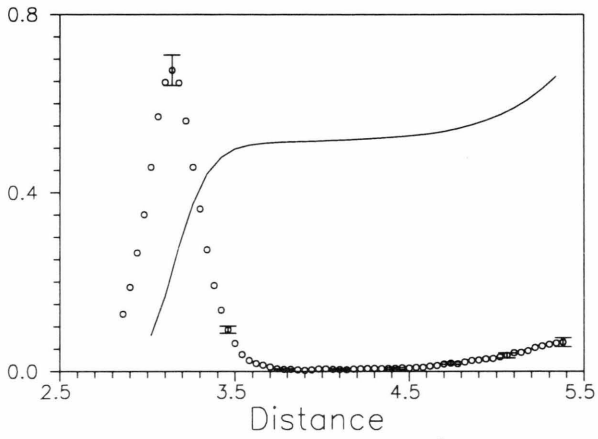

Fig. 6. Radial distribution function $g_{Li^+Li^+}(r/Å)$, and running integration number.

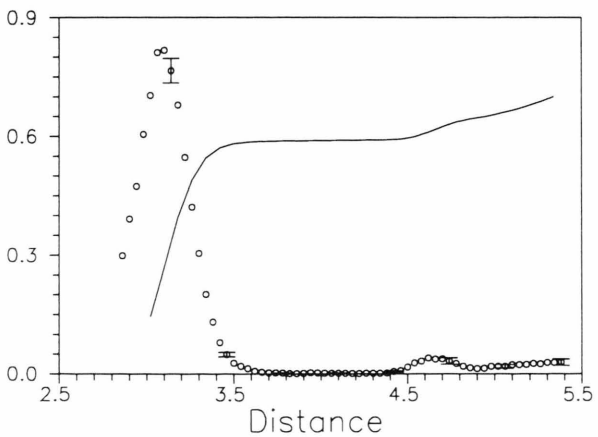

Fig. 7. Radial distribution function $g_{F^-F^-}(r/Å)$, and running integration number.

ion is involved in the local hydration structure. Accordingly, the plateaus in the running integration numbers tend to disappear and the boundaries between the first and second hydration shells become less well defined. These phenomena can also be observed by increasing the ion size [19] or by increasing the salt concentration [24]. Tanaka et al. [24] have shown that the cation enters the hydration shell of the anion as a consequence of ion pair formation. Some of the oxygen atoms in the first hydration shell of the lithium ion then simultaneously belong to the anionic shell. This results in an increase of the average anion-oxygen distance compared with the undisturbed case. The curves in Figs. 1–4 do not agree with the results obtained from Monte Carlo calculations [9], where the hydration structure appears much stronger.

Even though the SPC-FP model for pure water underestimates the bulk liquid structure [32], it can provide insight about the difference between the Monte Carlo and the present MD results. The discrepancy is probably caused by the polarization effect present in the SPC-FP model. This tends to destroy the normal hydrogen bonds of neighboring water molecules when the liquid is perturbed by added ionic solutes. One of the characteristics of the resulting many-body interactions is that a local breakdown of hydrogen bonding structure may cause a further breakage of neighboring hydrogen bonds [46].

Illustrated in Figs. 5–7 are ion-ion RDFs. All of these show a strong structure. A very sharp peak in $g_{Li^+F^-}(r)$ around 1.68 Å, which is slightly larger than the gas phase equilibrium bond length of 1.55 Å, indicates a predominance of ion pairs in the salt solution. A fluorine ion replaces a water molecule in the first hydration shell of Li^+. It can be estimated from the first minimum of $g_{Li^+F^-}(r)$ and from the running integration number plotted in the same figure that on average each ion is in contact with around 0.94 counterions. The first peaks in $g_{Li^+Li^+}(r)$ and $g_{F^-F^-}(r)$ are seen to be positioned slightly above 3 Å. This is within the molecular size of a water molecule and must therefore correspond to a configuration where two Li^+ or two F^- are coordinated to the same water molecule. These peaks almost coincide with the second peak of the Li^+–F^- RDF. In conclusion, neither cations nor anions in the 1.791 molal solution are uniformly distributed in the solution. Rather, their concentrations tend to bunch up because of the strong mutual interactions caused by the small ionic size. This is probably the main reason for the low solubility of LiF in water.

Table 2. Molecular geometry.

⟨O–H⟩ (Å)		⟨H–O–H⟩ (degrees)	
Solution	Pure water*	Solution	Pure water
0.971	0.966	101.0	101.0

* Data for pure water are from [32].

4. Geometry and Orientation of Water Molecules

The use of a flexible model permits the investigation of the influence of the ions on the geometry and vibrational characteristics of water molecules. Table 2 indicates an increase in the average O–H bond length, showing that the interaction between these ions and water is generally stronger than water-water interactions. There is no significant change in the H–O–H bond angle. Heinzinger [19] has pointed out that the repulsive forces exerted by a positive ion on the hydrogens, and the attractive ones of the oxygens, tend to decrease the bond angles of the hydration water molecules in the cationic shell. This role, however, is greatly diminished in a concentrated solution, such as the one studied here, by the existence of an anion in the same shell.

Figure 8 depicts $\cos\theta$ distributions, considering the first hydration shells of cation and anion. Here, θ is defined as the angle between the dipole moment direction of a water molecule and the vector pointing from the oxygen atom toward the center of the ion. For Li^+ the distribution shows a peak around $\cos\theta = -0.7$, corresponding to the orientation of a water lone pair towards the cation. On the other hand, preference for the formation of linear hydrogen bonds with the negative ion, observed in aqueous electrolyte solutions where contact ion pairs are scarce [19], practically disappears in the system studied here and gives rise to a strong tendency towards a uniform distribution of $\cos\theta$. Keep in mind that the hydration shell of F^- contains almost the entire shell of Li^+. A small peak located at $\cos\theta = 1$ indicates the possible formation of bifurcated hydrogen bonds with the anion.

Figure 9 illustrates the average value of $\cos\theta$ as a function of the distance of the oxygen atom to the lithium and fluorine ions. It is clear that the water molecules in the first hydration shell of Li^+ have a preference for occupying tetrahedral sites. Beyond this region, the preferential orientation of the water molecules decreases rapidly and drops to nil at the first

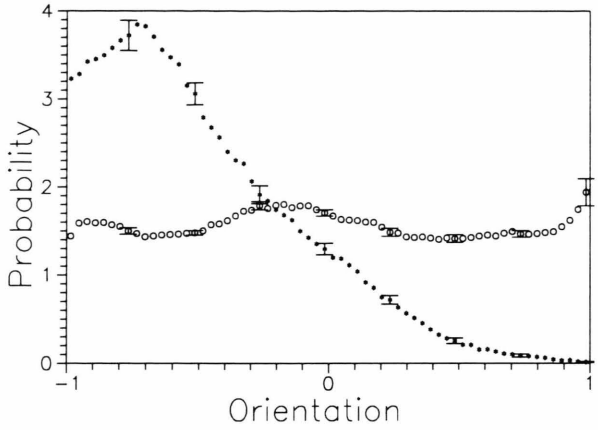

Fig. 8. Orientational ($\cos\theta$) distribution of the water molecules. Asterisks: in the first hydration shell of Li^+; circles: in the first hydration shell of F^-.

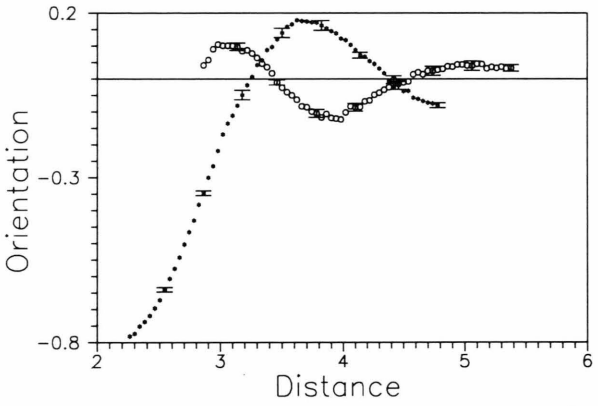

Fig. 9. Average $\cos\theta$ as a function of the distance (in Å) between ion and oxygen atom. Asterisks for Li^+, and circles for F^-.

minimum of the Li^+–O RDF. A second region of preferential water orientation is evident. This corresponds to the second, widely spread, peak of $g_{Li^+O}(r)$. From Fig. 9 one can see too that, even in the vicinity of a halide ion, linear hydrogen bonding to water may not be preferred if the halide ion is in close contact with an alkali ion. Perturbations from the latter become very significant.

5. Static Properties

Some thermodynamic and static dielectric properties of the solution are summarized in Table 3. For comparison, values, when available, of the corre-

Table 3a. Internal energies (in units of kcal/mol).

U_{WW}	U_{IW}	U_{II}	U_{sol}	$U_{pure\ water}$
−9.03 ±0.05	−33.07 ±1.60	−225.71 ±2.79	−16.33 ±0.05	−9.81

Table 3b. Dipole moments and Kirkwood g-factors.

μ_{sol}(Debye)	μ_{water}(Debye)	G_K(solution)	G_K(pure water)
2.57 ± 0.01	2.44	2.06 ± 0.26	2.65

sponding quantities found for pure water [32] are listed as well. It is evident that the Kirkwood finite-system g-factor, G_K [36], from which equilibrium fluctuations of the total dipole moment of the sample can be assessed, is lowered by ~20%. Accordingly, the average dipole moment per molecule is raised from 2.44 Debye to 2.57 Debye, and the solution, as evidenced from its internal energy, is about 60% more stable than pure water liquid. In a salt solution, the internal energy is comprised of water-water interactions, ion-water interactions and ion-ion interactions. For reference, the values of these components are contained in Table 3a. The average water-water interaction in the ionic solution is weaker than that in pure water because of the occupied space taken up by the ions.

6. Dynamical Motions

Impey et al. [3] have shown that the velocity autocorrelation function for Li^+ has the appearance of a damped oscillation characterized by a single frequency. This feature also exists for the present system as depicted in Figure 10. However, the oscillatory frequency is even higher and the damping even more rapid than in [3]. This is attributed to the participation of the halide ion for which the velocity autocorrelation function oscillates with the same frequency. It is natural to ascribe this high frequency motion to the rattling of the ion pair in a cage of solvent molecules. Of course, perturbations from the ions in nearby salt molecules may also influence this motion. Also displayed in Fig. 10 is the velocity autocorrelation function of the 248 solvent molecules, which does not show a high fre-

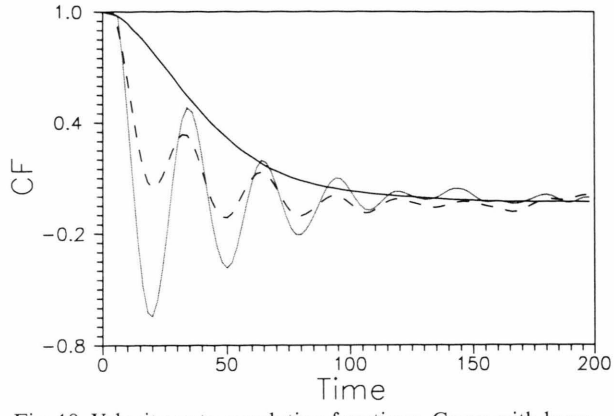

Fig. 10. Velocity autocorrelation functions. Curve with large oscillations: Li^+; broken curve: F^-; solid curve: center of mass of water molecules in solution. Time in units of fs.

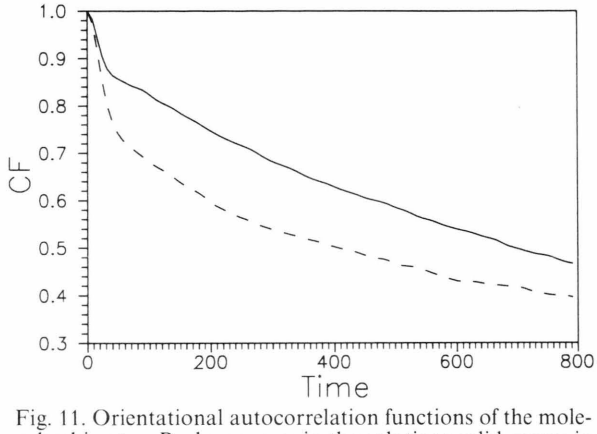

Fig. 11. Orientational autocorrelation functions of the molecular bisector. Broken curve: in the solution; solid curve: in pure liquid. Time in units of fs.

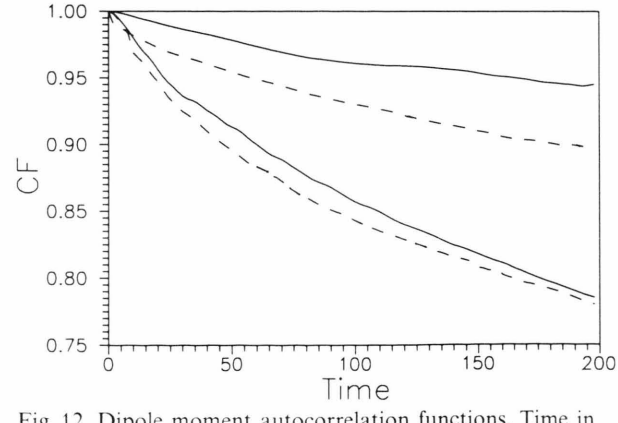

Fig. 12. Dipole moment autocorrelation functions. Time in units of fs. Upper curves for collective quantities; lower curves for single molecular quantities. Broken curves for water molecules in solution; solid curves for pure water.

Table 4. Intramolecular vibrational frequencies (cm^{-1}) [a].

	Bending	Symmetric stretching	Asymmetric stretching
Pure water	1802	3875	4080
Solution	1812	3653	3861
Δ(W–S)	−10	+222	+219

[a] The calculated frequencies are too high compared with corresponding experimental data in pure liquid water (1594.6, 3656.7, and 3755.8 cm^{-1}) because of the intramolecular potential model used in this calculation. We feel however that the calculated shifts should be reliable to within $\pm 50\ cm^{-1}$.

quency oscillation. The long negative tail indicates that the motion of the coordination shell is strongly hindered. The shape of this function must certainly be affected by the oscillatory motion of the ion pairs.

Figure 11 compares the orientational autocorrelation functions of the dipole of the water molecules in the ionic solution and in the pure liquid. The shape of this function provides evidence that the general breakage of hydrogen bonds causes a faster molecular orientational relaxation. This is in agreement with the experimental results of Hertz et al. [47], who have found that the water molecules in the first hydration shell of Li^+ rotate faster compared with the other water molecules. A similar speed-up of the dielectric relaxation caused by the ionic impurities can be observed in Figure 12.

Information on the intramolecular vibrational motions of hydration water can be obtained through Fourier transformation of the normalized velocity autocorrelation functions of the hydrogen atoms [48]. Table 4 presents the wave number shifts in the H–O–H bending and O–H stretching vibrations from the simulation results for the ionic solution and for pure water [32]. While the frequency change in the bending motion is found to be only $10\ cm^{-1}$, which is well within the limits of the computational error, a large red shift of the O–H stretching frequencies is observed. This effect has also been observed by other authors in very highly concentrated solutions, especially in solutions containing divalent cations [18, 23]. This observation indicates a strong influence of the ion pair on the intramolecular vibrations of the water molecules. The frequency splitting between the symmetric and asymmetric modes is seen to be insensitive to the addition of ions to water. This result again is in agreement with the conclusions of Bopp [23].

7. Concluding Remarks

In order to study the structure and properties of a 1.791 molal aqueous LiF solution, we have carried out a molecular dynamics computer simulation, using a flexible and polarizable water model. In such a concentrated solution, part of the hydration shell of a Li^+ ion belongs to the hydration shell of F^-. This phenomenon, in conjunction with the polarization effect, which tends to break chain-like hydrogen bonds, greatly reduces the hydration structure. On the average, the ion-water distances are larger than those for dilute systems. It is found that the lone pair of the hydration water in the cationic shell has a preference to occupy tetrahedral sites, while the orientation of the water molecules in the anionic shell is quite uniformly distributed. These water molecules form a cage around the ion pair so that the velocity autocorrelation functions for Li^+ and F^- oscillate with the same frequency. Because of the general breakage of hydrogen bonds in the aqueous solution, the orientational relaxation of the molecular dipole is faster than that in bulk water. A similar behavior can be observed in the correlation functions of the molecular dipole moment and the collective dipole moment. With the aid of the flexible model, we were also able to investigate intramolecular vibrational motions. A red shift in the O–H stretching modes, accompanied by an elongation of the corresponding bonds, occurs in the ionic solution.

Acknowledgements

Financial support at the SPQR Laboratory has been shared by the Robert A. Welch Foundation (D-0005, 39% and D-1094, 5%), the State of Texas Advanced Research Program (003644-004, 36%) and the Pittsburgh Supercomputing Center (20%).

[1] E. Clementi and R. Barsotti, Chem. Phys. Lett. **59,** 21 (1978).
[2] M. Mezei and D. L. Beveridge, J. Chem. Phys. **74,** 6902 (1981).
[3] R. W. Impey, P. A. Madden, and I. R. McDonald, J. Phys. Chem. **87,** 507 (1983).
[4] P. Pereg, W. K. Lee, and E. W. Prohofsky, J. Chem. Phys. **79,** 388 (1983).
[5] D. G. Bounds, Mol. Phys. **54,** 1335 (1985).
[6] S.-S. Sung and P. C. Jordan, J. Chem. Phys. **85,** 4045 (1986).
[7] E. Guàrdia and J. A. Padró, J. Phys. Chem. **94,** 6049 (1990).
[8] R. O. Watts, E. Clementi, and J. Fromm, J. Chem. Phys. **61,** 2550 (1974).
[9] K. Heinzinger and P. C. Vogel, Z. Naturforsch. **29a,** 1164 (1974).
[10] J. Fromm, E. Clementi, and R. O. Watts, J. Chem. Phys. **62,** 1388 (1975).
[11] P. C. Vogel and K. Heinzinger, Z. Naturforsch. **30a,** 789 (1975).
[12] K. Heinzinger and P. C. Vogel, Z. Naturforsch. **31a,** 463 (1976). – P. C. Vogel and K. Heinzinger, Z. Naturforsch. **31a,** 476 (1976).
[13] G. Palinkas, W. O. Riede, and K. Heinzinger, Z. Naturforsch. **32a,** 113 (1977).
[14] Gy. I. Szasz and K. Heinzinger, Z. Naturforsch. **34a,** 840 (1979).
[15] T. Radnai, G. Palinkas, Gy. I. Szasz, and K. Heinzinger, Z. Naturforsch. **36a,** 1076 (1981).
[16] W. Dietz, W. O. Riede, and K. Heinzinger, Z. Naturforsch. **37a,** 103 (1982).
[17] Gy. I. Szasz and K. Heinzinger, Z. Naturforsch. **38a,** 214 (1983).
[18] K. Heinzinger, Physica **131B,** 196 (1985).
[19] K. Heinzinger, Pure & Appl. Chem. **57,** 1031 (1985).
[20] M. M. Probst, T. Radnai, K. Heinzinger, P. Bopp, and B. M. Rode, J. Phys. Chem. **89,** 753 (1985).
[21] M. F. Mills, J. R. Reimers, and R. O. Watts, Mol. Phys. **57,** 777 (1986).
[22] M. Migliore, S. L. Fornili, E. Spohr, G. Palinkas, and K. Heinzinger, Z. Naturforsch. **41a,** 826 (1986).
[23] P. Bopp, Pure & Appl. Chem. **59,** 1071 (1987).
[24] K. Tanaka, N. Ogita, Y. Tamura, I. Okada, H. Ohtaki, G. Palinkas, E. Spohr, and K. Heinzinger, Z. Naturforsch. **42a,** 29 (1987). – L. X. Dang and B. M. Pettitt, J. Phys. Chem. **94,** 4303 (1990).
[25] R. W. Gurney, Ionic Processes in Solutions, McGraw-Hill, New York 1953.
[26] T. Erdey-Gruz, Transport Phenomena in Aqueous Solutions, Hilger, London 1974.
[27] R. M. Glaeser and B. K. Jap, Biophys. J. **45,** 95 (1984).
[28] F. H. Stillinger and C. W. David, J. Chem. Phys. **69,** 1473 (1978).
[29] P. Barnes, J. L. Finney, J. D. Nicholas, and J. E. Quinn, Nature London **282,** 459 (1979).
[30] J. Goodfellow, Proc. Natl. Acad. Sci. USA **79,** 4977 (1982).
[31] P. Perez, W. K. Lee, and E. W. Prohofsky, J. Chem. Phys. **79,** 388 (1983).
[32] S.-B. Zhu, S. Yao, J.-B. Zhu, and G. W. Robinson, J. Phys. Chem., in press.
[33] Handbook of Chemistry and Physics, 71th ed., CRC Press, Baca Raton, FL, 1990.
[34] K. Toukan and A. Rahman, Phys. Rev. **31B,** 2643 (1985).
[35] W. S. Benedict, N. Gailar, and E. K. Plyler, J. Chem. Phys. **24,** 1139 (1956).
[36] M. Neumann, J. Chem. Phys. **82,** 5663 (1985); **85,** 1567 (1986).
[37] E. A. Moelwyn-Hughes, Physical Chemistry, 2nd ed., Macmillan, New York 1964.
[38] M. Sprik and M. L. Klein, J. Chem. Phys. **89,** 7556 (1988).
[39] P. Ahlström, A. Wallqvist, S. Engström, and B. Jönsson, Mol. Phys. **68,** 563 (1989).
[40] P. Cieplak, P. Kollman, and T. Lybrand, J. Chem. Phys. **92,** 6755 (1990).
[41] D. Eisenberg and W. Kauzmann, The Structure and Properties of Water, Oxford University Press, New York 1969.
[42] F. G. Fumi and M. P. Tosi, J. Phys. Chem. Solids **21,** 31 (1964). – M. P. Tosi and F. G. Fumi, J. Phys. Chem. Solids **21,** 45 (1964).
[43] M. Born and J. E. Mayer, Z. Physik **75,** 1 (1932).
[44] L. Brewer and E. Brackett, Chem. Rev. **66,** 425 (1961).
[45] M. P. Allen and D. J. Tildesley, Computer Simulation of Liquids, Clarendon Press, Oxford 1987.
[46] S.-B. Zhu and G. W. Robinson, Proc. Internat. Conf. Supercomp. **II,** 189 (1989).
[47] H. G. Hertz, R. Tutsch, and H. Versmold, Ber. Bunsenges. **76,** 1177 (1971).
[48] G. C. Lie and E. Clementi, Phys. Rev. **33A,** 2679 (1986).